# Physical Properties of Oriented Poly(butylene Terephthalate)

W. P. LEUNG and C. L. CHOY, *Department of Physics, The Chinese University of Hong Kong, Hong Kong*

## Synopsis

The effect of orientation on the low-strain mechanical properties, dielectric relaxation, and thermal expansivity of poly(butylene terephthalate) has been studied. The $\alpha$ relaxation at 50°C (1 Hz), which involves large-scale chain motion in the amorphous regions, is reduced in magnitude and shifted to higher temperature after drawing. In contrast, the localized motions of the carbonyl and glycol groups associated with the $\beta$ process at −90°C (1 Hz) is not much affected by orientation. At low temperature, a large difference along and normal to the draw direction is observed for both Young's modulus and thermal expansivity. The anisotropy, however, diminishes with increasing temperature and becomes nearly zero above the $\alpha$ relaxation. This feature can be understood on the basis of the Takayanagi model.

## Introduction

Although poly(butylene terephthalate) (PBT) has become one of the most important engineering thermoplastics in recent years, there have been relatively few studies of the physical properties of this polymer. Early investigations[1,2] of the molecular motion by dynamic mechanical measurements reveal two relaxations. The $\alpha$ relaxation at 50°C (1 Hz) has been associated with the micro-Brownian motions of the chains in the amorphous regions whereas the $\beta$ relaxation at −90°C (1 Hz) involves more restricted motions of the carbonyl group and glycol residue. Recently, Chang and Slagowski[3] studied the effect of crystallinity and glass fiber reinforcement on the dynamic mechanical behavior, and found that the magnitude of both the $\alpha$ and $\beta$ relaxations decreases with increasing crystallinity, indicating that the limited motions of the carbonyl and glycol groups occur at least partly in the amorphous regions. Dielectric relaxation techniques[4–6] have also been used to study molecular motion in PBT. In particular, Ito and Kobayashi[6] have investigated the effect of water absorption on the $\beta$ relaxation.

Apart from the study by Ward et al.[7] on the tensile stress–strain behavior of oriented fibers of PBT, there has been no systematic investigation of the effect of orientation on the physical properties. To fill this gap, we report herein the results of our studies on the dynamic mechanical and dielectric behavior and the thermal expansivity of oriented PBT.

Journal of Applied Polymer Science, Vol. 27, 2693–2709 (1982)
 CCC 0021-8995/82/072693-17$02.70

## EXPERIMENTAL

### Sample Preparation and Characterization

The PBT used in this study was manufactured by BASF under the trade name Ultradur B4500 and was supplied in the form of sheets 3 mm thick. In order to prepare samples of different crystallinities, a 0.6 mm thick sheet was melted and then quenched in ice water while other sheets were annealed at 200°C for 36 h. The quenched samples were translucent whereas the as-received and annealed samples were opaque. Oriented samples were prepared by drawing the as-received sheets (gauge length 4 cm) at 120°C and a rate of 1 cm·min$^{-1}$ on an Instron Tensile Machine. PBT showed necking behavior, and only samples of one draw ratio ($\lambda = 3.3$) were obtained. All samples were stored at room temperature for at least 2 days before measurements were undertaken.

The densities of PBT samples were obtained by the flotation method and their volume fraction crystallinities $\chi$ were calculated from the relation

$$\chi = (\rho - \rho_a)/(\rho_c - \rho_a)$$

where $\rho$, $\rho_a$, and $\rho_c$ are the densities of the sample, the amorphous regions, and the crystalline regions, respectively. Taking $\rho_a = 1.280$ and $\rho_c = 1.396$,[8] the crystallinities of the quenched, as-received, annealed, and oriented samples were found to be 0.1, 0.31, 0.48, and 0.28 respectively.

### X-Ray Diffraction and Birefringence Measurements

Wide angle X-ray diffraction photographs were taken in transmission mode using a Phillips Camera and filtered CuK$\alpha$ radiation. The birefringence of the oriented sample was measured with a Leitz polarizing microscope equiped with a tilting compensator.

### Mechanical Measurements

Dynamical torsional measurement at 1 Hz was carried out on a torsional pendulum of the inverted type similar to that of Gray and McCrum.[9] Dynamic tensile measurements between 5 and 90 Hz were made on a viscoelastic spectrometer (Iwamoto Seisakusho Ltd.). For oriented samples, torsional measurements were made only about the draw axis whereas tensile measurements were made both along and normal to the draw axis. These measurements covered the range −170–140°C.

Ultrasonic measurements at 2.5 MHz were carried out between −70°C and 130°C using a liquid tank method similar to that of Rawson and Rider.[10] The experimental detail has been described in a previous publication.[11] All five independent moduli, namely, $C_{11}$, $C_{12}$, $C_{13}$, $C_{33}$, and $C_{44}$ as well as tan $\delta$ in the direction perpendicular to the draw axis were obtained.

### Dielectric Measurement

An Ando transformer ratio arm bridge was used in the dielectric relaxation measurements at frequencies ranging from 30 Hz to 1 MHz at temperatures between −120°C and 120°C.

The complex dielectric constants of oriented PBT were measured both with the electric field parallel and perpendicular to the draw axis. When the electric field is perpendicular to the draw axis, the sample is a thin sheet with the draw axis lying in the plane of the sheet. For an electric field parallel to the draw axis, the sample is prepared by cutting 2 mm wide strips from the oriented PBT sheet perpendicualr to the draw direction, then turning through 90°, and placing them side by side to achieve the required size. These strips were then tightened by cotton threads. Since there are air spaces between the strips, corrections have to be made in the calculation of dielectric constants. Details regarding the experiment and data analysis can be found elsewhere.[12]

### Thermal Expansivity Measurement

Thermal expansivity measurements along and normal to the draw axis were made between −150°C and 120°C on a Perkin-Elmer thermomechanical analyzer TMS 2 at a heating rate of 10 K·min$^{-1}$. The procedure and data analysis have been described in detail previously.[13] The thermal expansivity is physically meaningful only if the dimensional changes are reversible. To prevent irreversible thermal shrinkage, the oriented sample was annealed for 1 h at 125°C, i.e., 5°C above the upper temperature limit, before the measurement.

## RESULTS AND DISCUSSIONS

### X-Ray Diffraction and Birefringence

Although the effect of orientation on the structure of other semicrystalline polymers such as polyethylene[14] and poly(ethylene terephthalate)[15,16] has been studied in great detail, there is very little information on PBT.[17] Analogous to other polymers, we expect that the chains in both the crystalline and amorphous regions of oriented PBT are preferentially aligned along the draw direction, with the chains in the crystalline regions showing a higher degree of orientation. There may also be some taut tie-molecules connecting the crystalline blocks.

It is well established[18] that, for oriented PBT not under tension, the crystalline regions are in the $\alpha$-form, i.e., the chains are only 86% extended. When the sample is stretched about 12% along the draw direction, the crystals transform into the $\beta$-form, in which the chain is close to its fully extended length. The wide-angle X-ray patterns of the isotropic and oriented PBT samples used in our study (Fig. 1) reveal that the crystalline regions are in the $\alpha$-form and there is a high degree of chain orientation after drawing.

The birefringence $\Delta$ of the oriented sample is 0.149. Neglecting form birefringence, $\Delta$ can be expressed as

$$\Delta = \chi f_c \Delta_c^0 + (1 - \chi) f_a \Delta_a^0 \tag{1}$$

where $\Delta_c^0$ and $\Delta_a^0$ are the intrinsic birefringences of the crystalline and amorphous regions, respectively, and $f_c$ and $f_a$ are the crystalline and amosphous orientation functions, respectively. Unfortunately, $\Delta_c^0$ and $\Delta_a^0$ for PBT are not known, but, for a crude estimate, the corresponding values $\Delta_c^0 = 0.220$ and $\Delta_a^0 = 0.275$ [16] for poly(ethylene terephthalate) will be used. Assuming $f_c \sim 0.7$ (as judged roughly from the X-ray photographs), $f_a \sim 0.5$, indicating appreciable chain orientation in the amorphous regions.

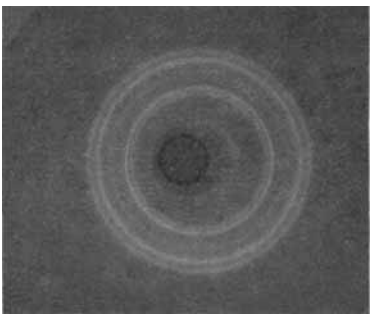

(a)

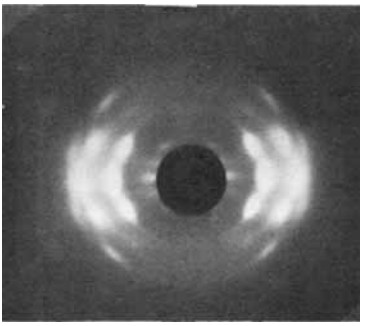

(b)

Fig. 1. Wide angle X-ray patterns for PBT. (a) isotropic sample; (b) drawn ($\lambda = 3.3$) sample. CuK$\alpha$ line is used in taking these pictures. Draw axis vertical.

## Low-Frequency Mechanical Measurement

Since the mechanical properties are expected to depend on both crystallinity and orientation, we first discuss briefly the effect of crystallinity on the dynamic mechanical behavior. As shown in Figure 2(b), the temperature locations of the $\alpha$ and $\beta$ relaxations are independent of crystallinity, but the heights of both peaks decrease with increasing crystallinity. The $\alpha$ relaxation is associated with large-scale chain motions in the amorphous regions, so it is natural to observe a decrease in peak height with increasing crystallinity. A similar feature observed for the $\beta$ relaxation indicates that the limited motions of the glycol and carbonyl groups also occur at least partly in the amorphous regions. At low temperature, Young's modulus increases only by 30% as the crystallinity increases from 0.1 to 0.48, but since the sample with highest crystallinity has smaller drops at the two relaxations, its modulus at 90°C is much higher than the sample with $\chi = 0.1$.

The influence of orientation on the dynamic torsional behavior of PBT is shown in Figure 3. It is seen that the $\alpha$ peak is slightly suppressed and is shifted to higher temperature after drawing. This arises from the reduction in molecular mobility in the amorphous regions as a result of chain orientation and the presence of strained tie-molecules. The location of the $\beta$ relaxation remains unchanged and its magnitude is slightly enhanced by drawing, indicating that the limited motions of the glycol and carbonyl groups are only slightly influenced by molecular orientation.

At low temperature, the shear modulus $G$ is little affected by orientation. As a result of the enhancement of the $\beta$ process by drawing, $G$ for the oriented sample becomes lower than that for the isotropic sample just above the $\beta$ relax-

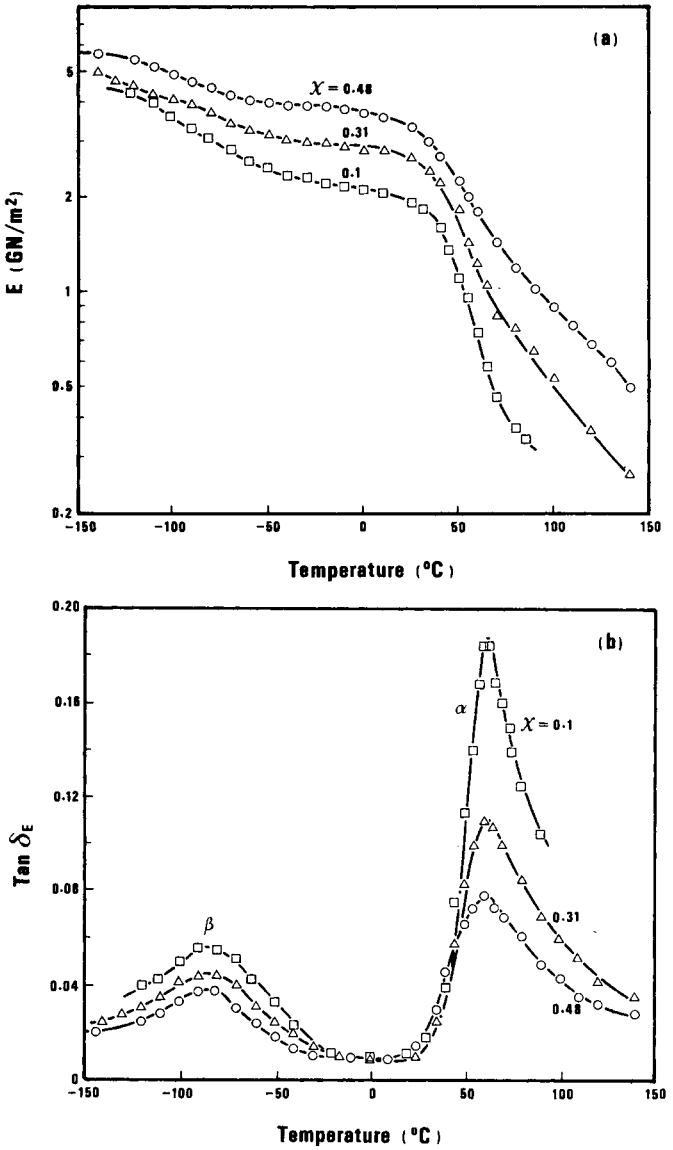


Fig. 2. Temperature dependence of (a) Young's modulus $E$ and (b) tan $\delta_E$ at 10 Hz for PBT at different crystallinities $\chi$.

ation. However, the fall in $G$ for oriented PBT at the $\alpha$ relaxation is smaller and occurs at higher temperature, so that there is a crossover in the shear moduli in this region.

As shown in Figure 4, the effect of orientation on the dynamic tensile behavior is quite similar. For the oriented sample, $\tan \delta_{\parallel} > \tan \delta_{\perp}$ for both the $\alpha$ and $\beta$ processes, i.e., the relaxation is stronger when the stress is applied along the draw direction. As a result, the anisotropy in Young's modulus, $E_{\parallel}/E_{\perp}$, is about 2 at low temperature, but it decreases to 1.1 at 140°C. This feature can be understood in terms of Takayanagi model,[19] assuming that the crystalline and amorphous regions in the oriented sample are arranged in series along the draw axis and in parallel in the perpendicular direction. Then the large anisotropy

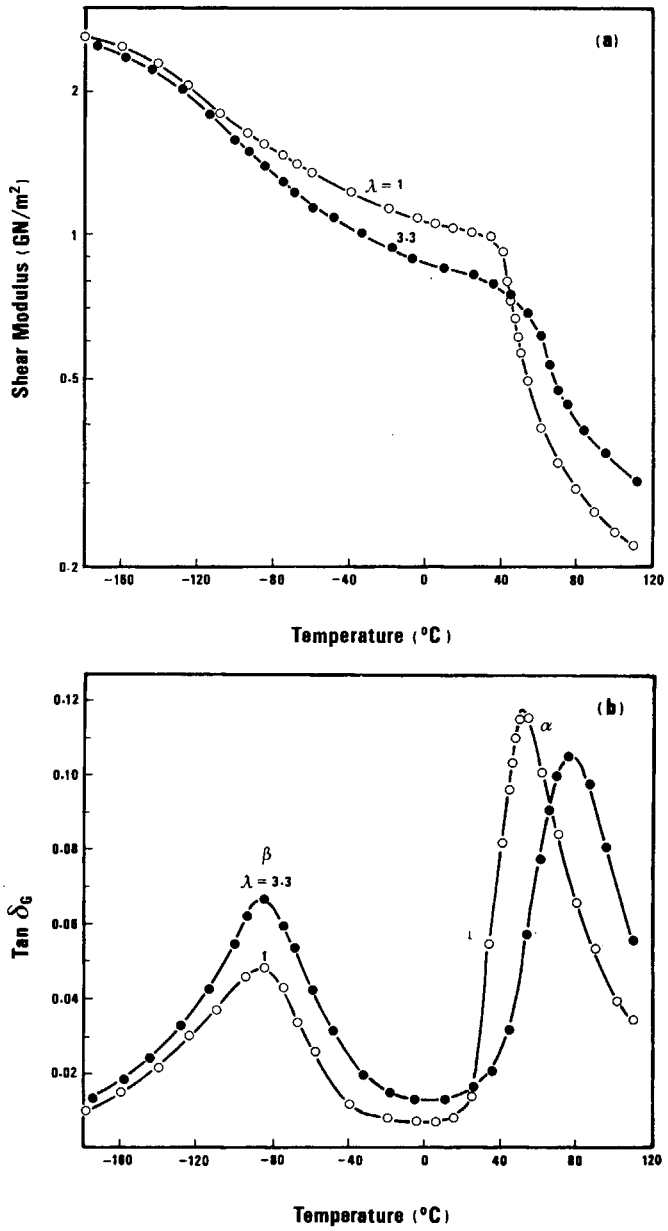


Fig. 3. Temperature dependence of (a) the shear modulus $G$ and (b) tan $\delta_G$ at 1 Hz for PBT: Isotropic (○) and oriented ($\lambda$ = 3.3) (●) samples.

at low temperature arises from chain orientation in both crystalline and amorphous regions. However, application of stress along the draw direction would give a large fall of modulus at the strong amorphous relaxation region ($\alpha$ process). In the perpendicular direction where the crystalline and amorphous regions are in parallel, the fall in modulus is smaller since the crystalline region still supports the applied stress. As a result, $E_{\parallel} \sim E_{\perp}$ above the $\alpha$ relaxation. However, the presence of a small number of taut tie-molecules in the amorphous regions prevents $E_{\parallel}$ from falling below $E_{\perp}$, as was observed for well-annealed samples of other polymers.[19]

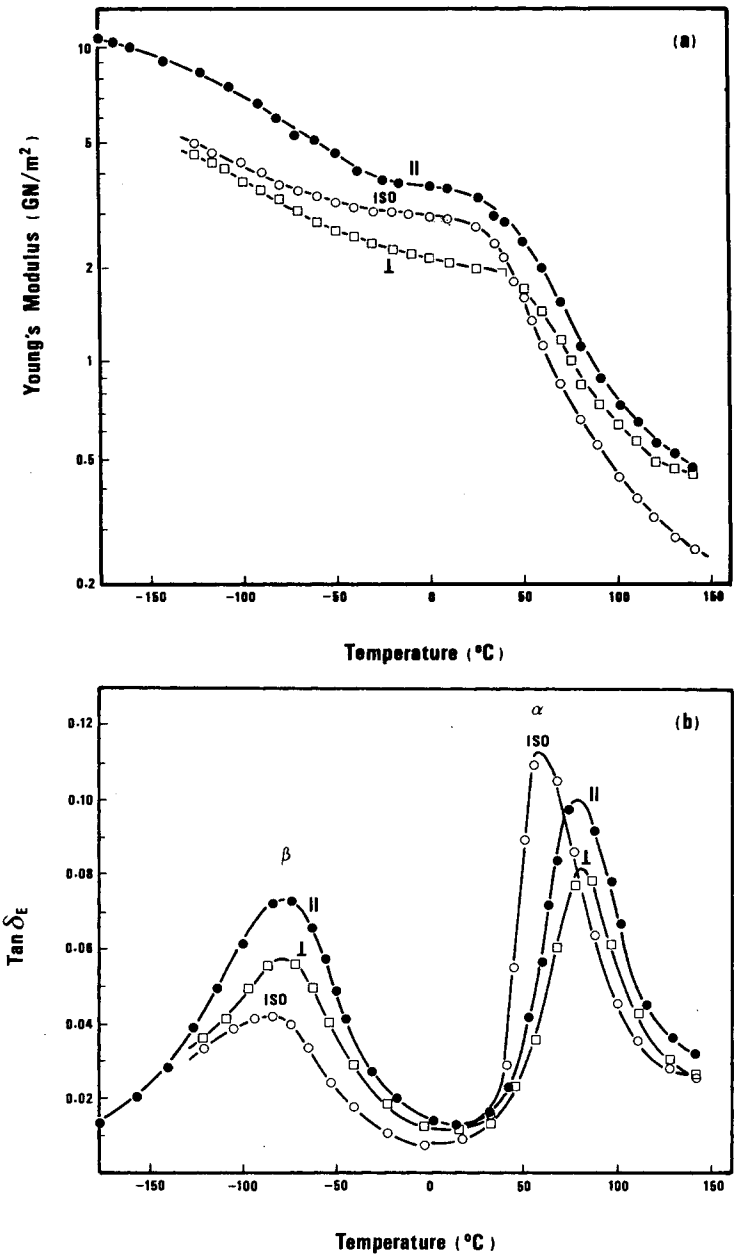


Fig. 4. Temperature dependence of (a) Young's modulus $E$ and (b) tan $\delta_E$ at 10 Hz for PBT: (●) measured along the draw direction; (□) measured perpendicular to the draw direction; (○) isotropic sample.

It is interesting to note that at the lowest temperature $E_{\parallel}$ has a value of 10.7 GN·m$^{-2}$. As we shall see, ultrasonic measurements at −70°C also give similar value (see Fig. 7). This is slightly larger than the theoretical value[20] of 10.1 GN·m$^{-2}$ for Young's modulus along the chain axis of a PBT crystal in $\alpha$-form and the observed value[20] of 8.7 GN·m$^{-2}$ obtained from the X-ray method. The X-ray determination of the crystal modulus is based on the assumption that the stress on the crystalline region is the same as the overall stress on the oriented

sample. This uniform stress assumption is normally not valid at room temperature and would lead to too low a value.[21] The theoretical value also seems somewhat low, and a more refined calculation is necessary to resolve this discrepancy.

## Ultrasonic Measurement

The loss tangent corresponding to 2.5 MHz longitudinal elastic wave propagating normal to the draw axis is shown as a function of temperature in Figure 5. As one would expect from the well-known time–temperature equivalence principle, both the $\alpha$ and $\beta$ relaxations in the isotropic sample are shifted to higher temperatures, with the $\beta$ peak shifting by a larger factor. This leads to large overlapping of the two peaks so that the $\beta$ peak appears only as a shoulder on the low-temperature side of the $\alpha$ peak. After drawing, the $\alpha$ peak is strongly suppressed because of the presence of taut tie-molecules in the amorphous regions; consequently, only a single broad composite peak is observed.

The low-strain mechanical properties of an unaxially oriented polymer is completely characterized by five stiffness constants $C_{11}$, $C_{12}$, $C_{13}$, $C_{33}$, and $C_{44}$, which can be determined by an ultrasonic method previously described.[11] The stiffness constants for both isotropic and oriented PBT are shown in Figure 6. The influence of temperature is different for different stiffness constants, with the shear moduli $C_{44}$ and $C_{66}$ showing the strongest temperature dependence and $C_{12}$ and $C_{13}$ decreasing only slightly with increasing temperature.

For the oriented sample at low temperature, the longitudinal modulus along the draw axis ($C_{33}$) is about twice that of the modulus ($C_{11}$) in the transverse direction, whereas the shear modulus in planes containing the draw axis ($C_{44}$) is 35% higher than the modulus in planes perpendicular to the draw axis, $C_{66}$ [= $\frac{1}{2}(C_{11} - C_{12})$]. These anisotropies arise from the fact that $C_{33}$ and $C_{44}$ involve

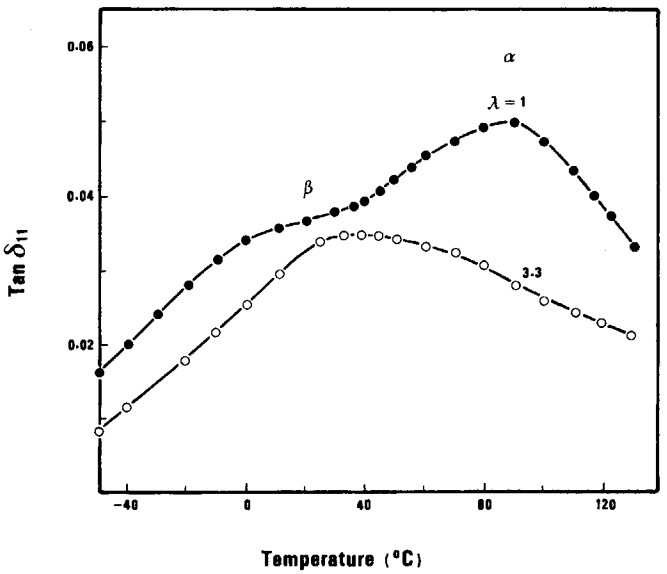


Fig. 5. Temperature dependence of the ultrasonic loss factor tan $\delta$ at 2.5 MHz for isotropic (●) and oriented ($\lambda$ = 3.3) (○) PBT. For the oriented sample, ultrasonic waves propagate in the direction normal to the draw axis.

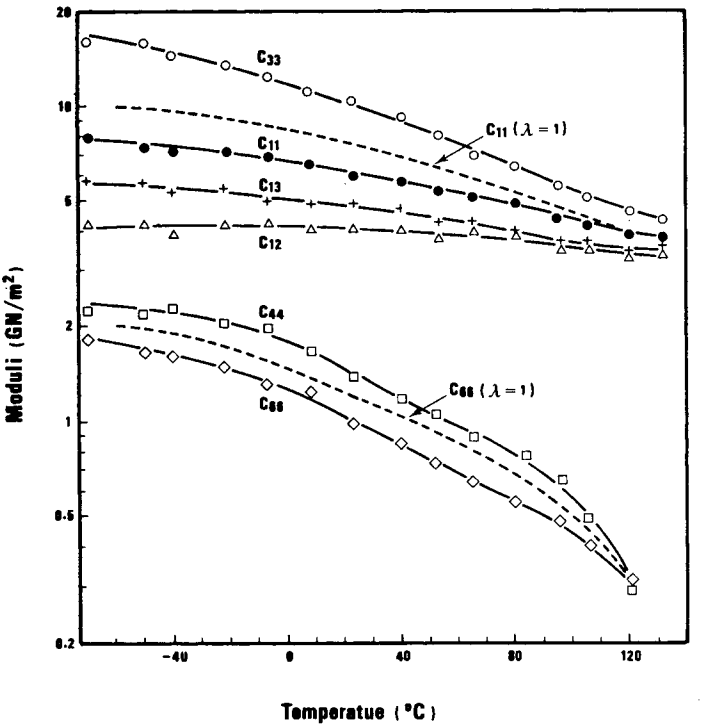


Fig. 6. Temperature dependence of the elastic moduli of oriented PBT ($\lambda = 3.3$). Among the six moduli, only five of them are independent ($C_{12} = C_{11} - 2C_{66}$). The elastic moduli of isotropic PBT, $C_{11}$ and $C_{66}$, are also shown (---).

the deformation of the strong covalent bonds, which are now largely aligned along the draw axis. The anisotropy, however, decreases with increasing temperature and becomes nearly zero at 130°C. The ultrasonic Young's moduli (Fig. 7) also

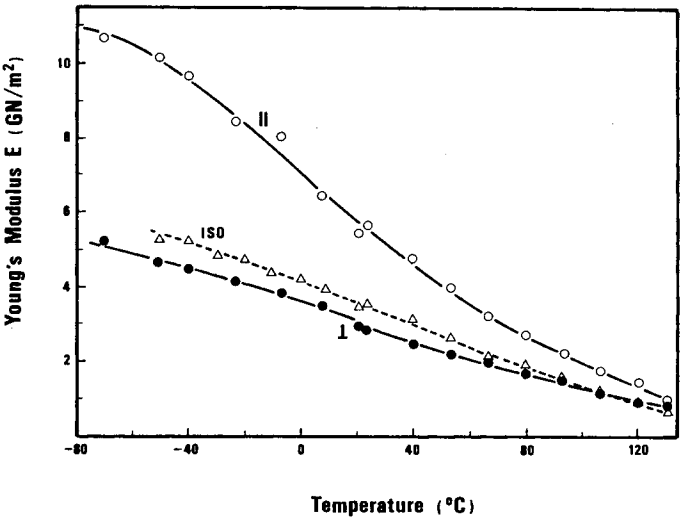


Fig. 7. Temperature dependence of Young's moduli $E_{\parallel}$, $E_{\perp}$ for oriented PBT and $E_{iso}$ for isotropic PBT, calculated from the measured $C_{ij}$.

exhibit this feature, which has earlier been observed in low-frequency tensile measurements [Fig. 4(a)] and explained in terms of the Takayanagi model.

## Dielectric Measurement

The dielectric constant and loss factor, $\epsilon'$ and $\epsilon''$ of the "as-received" sample ($\chi = 0.31$) at 110 Hz, 10 KHz, and 1 MHz are shown as functions of temperature in Figure 8. The $\alpha$ and $\beta$ peaks are again observed, and they shift upward in temperature as the frequency increases. Since the $\beta$ relaxation shows a much

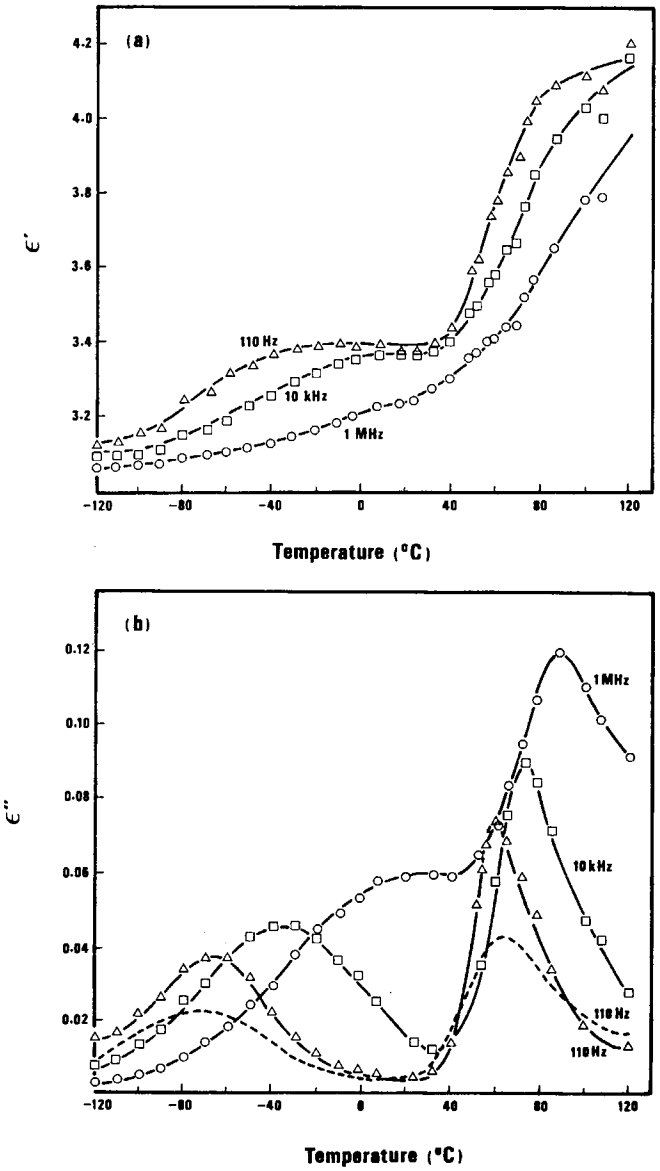


Fig. 8. Temperature dependence of (a) the dielectric constant $\epsilon'$ and (b) loss factor $\epsilon''$ for as-received PBT ($\chi = 0.31$) at different frequencies. The dielectric loss factor $\epsilon''$ at 110 Hz of an annealed sample ($\chi = 0.48$) is also shown (- - -) in (b).

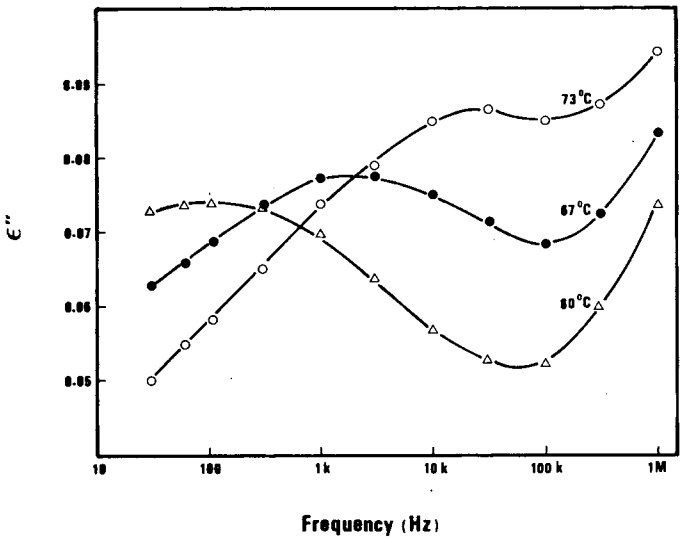


Fig. 9. Frequency dependence of the dielectric loss factor $\epsilon''$ at various temperature for as-received PBT in the $\alpha$ relaxation region.

larger shift, there is considerable overlapping of the two peaks at frequencies above 10 KHz. Figure 8 also shows the loss factor at 110 Hz for a sample of higher crystallinity ($\chi$ = 0.48). Similar to mechanical relaxations, both the $\alpha$ and $\beta$ peaks decrease in magnitude, but the peak positions remain unchanged.

The overlapping of the two relaxations can also be observed in the plots of loss factor vs. frequency shown in Figure 9. At 60°C, the $\alpha$ peak is located near 100 Hz. As the temperature increases, the $\alpha$ peak shifts to higher frequency and overlaps with the $\beta$ peak. Consequently, we have not been able to determine

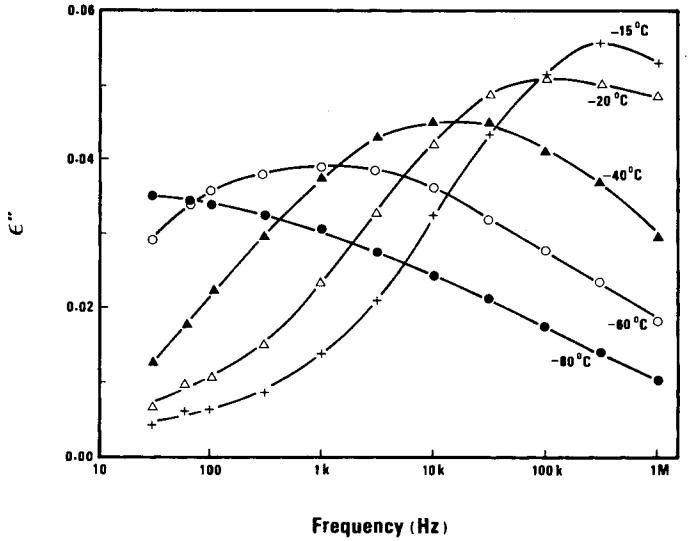


Fig. 10. Frequency dependence of the dielectric loss factor at various temperatures for as-received PBT in the $\beta$ relaxation region.

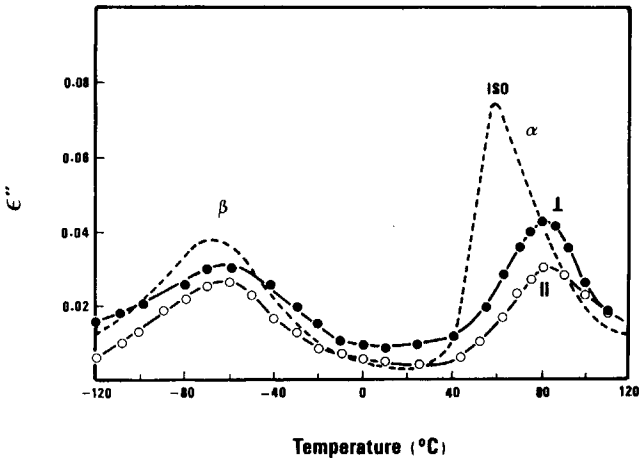


Fig. 11. Temperature dependence of the dielectric loss factor $\epsilon''$ for oriented PBT at 110 Hz. ($\perp$) measured with electric field normal to the draw axis; ($\parallel$) measured with electric field parallel to the draw axis. The loss factor $\epsilon''$ of the as-received isotropic sample is shown (---) for comparison.

the relaxation strength $\Delta\epsilon$ for the $\alpha$ process. The frequency plots of loss factor for the $\beta$ relaxation are shown in Figure 10. The relaxation strength $\Delta\epsilon$, obtained from Cole–Cole plots,[22] is roughly independent of temperature between $-1.5$°C and $-60$°C, and has an average value of 0.35.

Figure 11 reveals that the effect of orientation on the $\alpha$ relaxation is similar to the mechanical measurements (Figs. 3 and 4), i.e., the peak shifts up by about 25°C and becomes much smaller in magnitude, once again demonstrating the restraint on micro-Brownian chain motions in the amorphous regions. In contrast, the $\beta$ peak remains at about the same temperature and is only slightly suppressed.

At both relaxations, the loss factor ($\epsilon''_\perp$) for the sample with draw direction normal to the applied electric field is larger than that for draw direction parallel to the field ($\epsilon''_\parallel$). This anisotropy is consistent with the preferential alignment of chain molecules along the draw direction.[12,23] Similar features can also be seen in the frequency plots of the dielectric loss (Figs. 12 and 13). However, because of the large reduction in the magnitude of the $\alpha$ relaxation and the strong overlap of the $\alpha$ and $\beta$ processes, the $\alpha$ peak shows up only as a plateau in the low frequency region (Fig. 12). On the other hand, the $\beta$ relaxation is quite prominent. The relaxation strengths of the $\beta$ process, $\Delta\epsilon_\perp$ and $\Delta\epsilon_\parallel$, determined from Cole–Cole plots, are roughly temperature-independent and equal 0.40 and 0.23, respectively. The difference in the relaxation strength reflects the overall chain orientation in the drawn sample and can, in principle, provide a quantitative measure of molecular orientation.[12,23] It is, unfortunately, not possible to calculate the orientation function from these data since the angle between the dipole moment and the chain axis is not known.

## Activation Energy

Figures 14 and 15 show the plots of $\log f$ vs. $1/T$ for the relaxations in PBT, where $T$ refers to the temperature of maximum loss in constant frequency ($f$) experiments. For the $\alpha$ relaxation, two different curves are obtained—one for

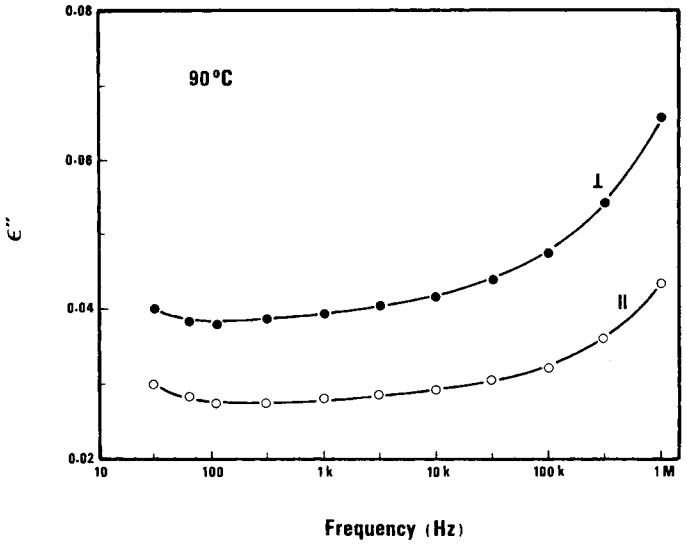


Fig. 12. Frequency dependence of $\epsilon''$ for oriented PBT at 90°C, showing the anisotropy in the $\alpha$ relaxation region when the electric field is applied along ($\parallel$) and perpendicular ($\perp$) to the draw direction.

the isotropic sample and the other for the drawn sample. Since this relaxation is associated with the glass transition, the curves should in general follow the WLF relation.[24] However, within the limited frequency range 0.1–300 KHz, the curves are roughly linear, giving activation energies of 67 and 110 kcal/mol for the isotropic and oriented samples, respectively. The oriented sample has much higher activation energy because of the constraint on micro-Brownian motions arising from chain orientation and the presence of taut tie-molecules. On the other hand, the $\beta$ relaxation is not much affected by orientation so that the activation energy for both samples is the same (13.1 kcal/mol). Since the $\alpha$ relaxation is associated with large scale motions of the chain backbones,

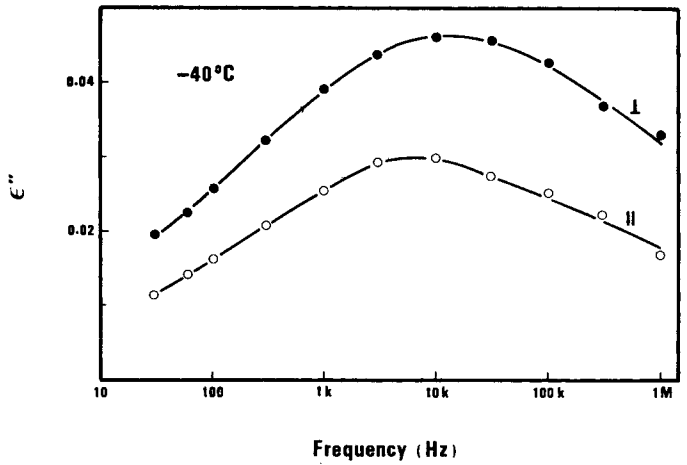


Fig. 13. Frequency dependence of $\epsilon''$ for oriented PBT at −40°C, showing the anisotropy in the $\beta$ relaxation region. Legends are same as in Figure 12.

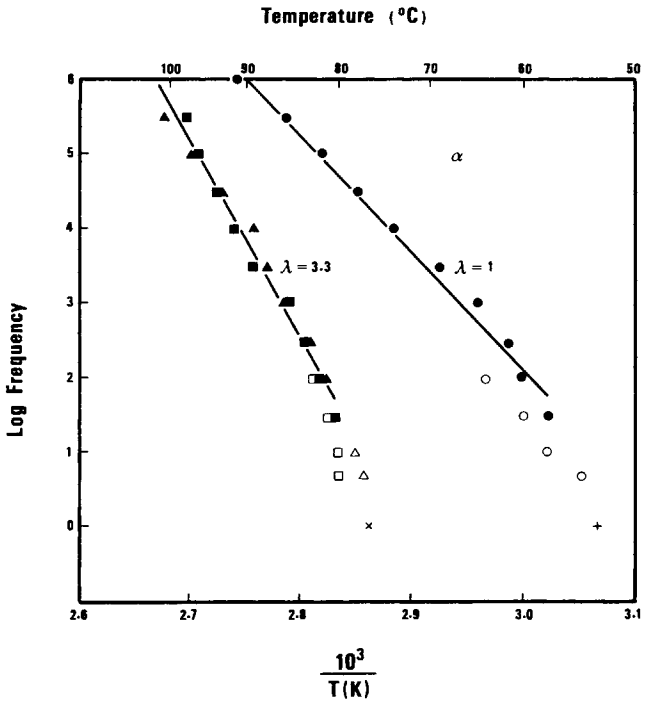


Fig. 14. Plots of log $f$ vs. $1/T$ for the $\alpha$ relaxation of isotropic and oriented PBT. Dielectric (●, ■, ▲) and dynamic tensile (○, □, △) data; (●, ○) isotropic; (▲, △) oriented ∥; (■, □) oriented ⊥. Dynamic torsional data: (+) isotropic; (×) oriented.

whereas the $\beta$ relaxation involves local motions of various chemical groups, it is reasonable that the activation energy of the $\alpha$ process is much higher than that of the $\beta$ process.

## Thermal Expansivity

On comparing the thermal expansivities of isotropic and oriented PBT in Figure 16, two interesting features are noteworthy. First, the glass transition temperature $T_g$ for the oriented sample is higher by about 25°C, consistent with the results of mechanical and dielectric relaxation. Second, at low temperature, the thermal expansivity along the draw axis ($\alpha_\parallel$) decreases drastically while the expansivity in the perpendicular direction ($\alpha_\perp$) increases only by 40%. This is in agreement with the results for other crystalline polymers[13,25] and arises from chain orientation and the presence of taut tie-molecules connecting the crystallites along the draw direction.

At −150°C, $\alpha_\perp$ is eight times larger than $\alpha_\parallel$, but $\alpha_\perp/\alpha_\parallel$ decreases with increasing temperature and becomes about 2 just below $T_g$. Moreover, $\alpha_\parallel$ shows a large jump at $T_g$ comparable to that of isotropic PBT, while $\alpha_\perp$ exhibits only a slightly faster rise. As a result, $\alpha_\parallel \sim \alpha_\perp$ above $T_g$, a behavior different from other crystalline polymers, which show anisotropy over the entire temperature range.[13,25]

The Takayanagi model can also give a satisfactory explanation for the difference in temperature dependence of $\alpha_\parallel$ and $\alpha_\perp$. The crystalline and amor-

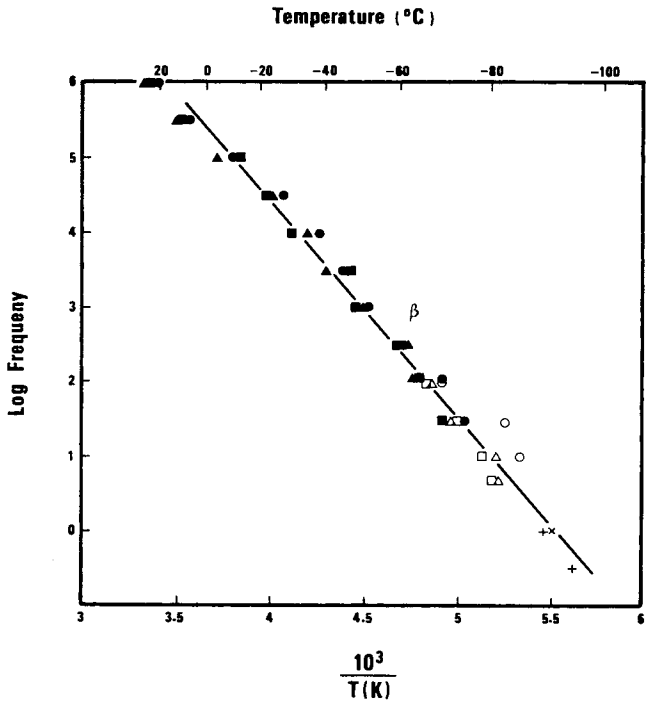


Fig. 15. Plot of log $f$ vs. $1/T$ for the $\beta$ relaxation of PBT. Legends are same as in Figure 14.

phous regions are connected in series along the draw direction, so $\alpha_{\parallel} = \chi\alpha_{\parallel}^{c} + (1 - \chi)\alpha_{\parallel}^{a}$, where $\alpha_{\parallel}^{c}$ and $\alpha_{\parallel}^{a}$ are, respectively, the thermal expansivities of the crystalline and amorphous regions along the draw direction. $\alpha_{\parallel}^{c}$ is expected to be small[25] since the crystalline chains are mostly aligned. Therefore, $\alpha_{\parallel}$ is dominated largely by $\alpha_{\parallel}^{a}$, which is quite small at $-150$°C owing to chain orientation in the amorphous region. However, $\alpha_{\parallel}^{a}$ has a large increase at the subglass transition ($\beta$ relaxation) and an even larger one at $T_g$, since the number of strained tie-molecules is not large enough to prevent free volume expansion. On the other hand, the crystalline and amorphous regions are connected in parallel in the perpendicular direction so that the expansion of the amorphous region is constrained by the crystalline region, and, consequently, no large jump at $T_g$ is observed.

## CONCLUSIONS

The process of drawing produces chain orientation in both the crystalline and amorphous regions and taut tie-molecules connecting the crystallites. This gives rise to considerable restriction on the large-scale chain motion associated with the $\alpha$ relaxation. On the other hand, the localized motions of the carbonyl and glycol groups at the $\beta$ relaxation are not much affected. Young's modulus and thermal expansivity measurements indicate that the mechanical and thermal anisotropy of oriented PBT at low temperature are quite large, but they diminish with increasing temperature and become almost zero above the $\alpha$ relaxation. This feature can be explained by the Takayanagi model, with the assumption that the crystalline and amorphous regions are arranged in series along the draw axis and in parallel in the transverse direction.

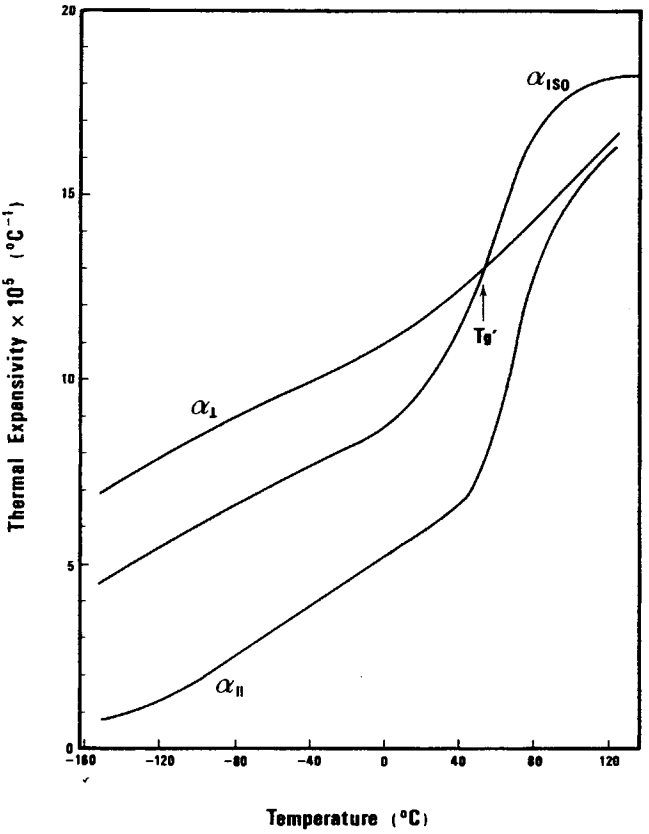


Fig. 16. Temperature dependence of the linear thermal expansivities of PBT. $T_g'$ denotes the glass transition for isotropic PBT.

## References

1. G. Farrow, J. McIntosh, and I. M. ward, *Makromol. Chem.*, **38**, 147 (1960).
2. K. H. Illers and H. Breuer, *J. Coll. Sci.*, **18**, 1 (1963).
3. E. P. Chang and E. L. Slagowski, *J. Appl. Polym. Sci.*, **22**, 769 (1978).
4. F. Sandrolini and P. Manaresi, *Conv. Ital. Sci. Macromol.*, 19 (1977).
5. G. A. Lushcheikin, V. S. Kolerov and M. K. Polevaya-Mansfel'd, *Plast. Massy.*, **10**, 65 (1976).
6. E. Ito and Y. Kobayashi, *J. Appl. Polym. Sci.*, **25**, 2145 (1980).
7. I. M. Ward, M. A. Wilding, and H. Brody, *J. Polym. Sci., Phys. Ed.*, **14**, 263 (1976).
8. A. Misra and R. S. Stein, *Bull. Am. Phys. Soc., Ser. II*, **20**, 341 (1975).
9. R. W. Gray and N. G. McCrum, *J. Polym. Sci. A-2*, **7**, 1329 (1969).
10. F. F. Rawson and J. G. Rider, *J. Phys. D: Appl. Phys.*, **7**, 41 (1974).
11. W. P. Leung, C. C. Chan, F. C. Chen, and C. L. Choy, *Polymer*, **21**, 1140 (1980).
12. C. L. Choy, K. H. Cheng, and B. S. Hsu, *J. Polym. Sci., Polym. Phys. Ed.*, **19**, 991 (1981).
13. C. L. Choy, F. C. Chen, and E. L. Ong, *Polymer*, **20**, 1191 (1979).
14. I. M. Ward, Ed., *Structure and Properties of Oriented Polymers*, Applied Science, London, 1975.
15. R. J. Samuels, *Structured Polymer Properties*, Wiley, New York, 1974.
16. J. H. Dumbleton, *J. Polym. Sci. A-2*, **6**, 795 (1968).
17. R. S. Stein and A. Misra, *J. Polym. Sci., Phys. Ed.*, **18**, 327 (1980).
18. R. Jakaways, I. M. Ward, M. A. Wilding, I. J. Desborough, and M. G. Pass, *J. Polym. Sci., Phys. Ed.*, **13**, 799 (1975).
19. M. Takayanagi, K. Imada, and T. Kajiyama, *J. Polym. Sci. C*, **15**, 263 (1966).
20. K. Tashiro, Y. Nakai, M. Kobayashi, and H. Tadokoro, *Macromolecules*, **13**, 137 (1980).

21. B. Brews, J. Clements, G. R. Davies, R. Jakaways, and I. M. Ward, *J. Polym. Sci., Phys. Ed.*, **17**, 351 (1979).
22. R. H. Cole and K. S. Cole, *J. Chem. Phys.*, **9**, 341 (1941).
23. B. S. Hsu and S. H. Kwan, *J. Polym. Sci., Phys. Ed.*, **14**, 1591 (1976).
24. M. L. Williams, R. F. Landel, and J. D. Ferry, *J. Am. Chem. Soc.*, **77**, 3701 (1955).
25. C. L. Choy, F. C. Chen, and K. Young, *J. Polym. Sci. Phys. Ed.*, **19**, 335 (1981).

Received December 11, 1981
Accepted January 18, 1982